# (Si and B)-Heterocyclic Carbenes and Theoretical Design of New Molecules


| | |
|---|---|
| Journal: | *Molecular Systems Design & Engineering* |
| Manuscript ID | ME-ART-07-2022-000138.R1 |
| Article Type: | Paper |
| Date Submitted by the Author: | 22-Aug-2022 |



| | |
|---|---|
| Complete List of Authors: | Tian, Zeqiong; Shaanxi Normal University, School of Chemistry & Chemical Engineering<br>Zhang, Congjie; Shaanxi Normal University, School of Chemistry & Chemical Engineering<br>Pei, Zhipeng; Flinders University<br>Liang, Jin-Xia; Guizhou University<br>Mo, Yirong; University of North Carolina at Greensboro, Naniscience |

**Design, System, Application Statement**

Carbenes have been playing a significant role in organic chemistry and considerable efforts have been spent to develop new types of carbenes. Inspired by the recent experimental work reported by Li et al. (*J. Am. Chem. Soc.* **2021,** *143*, 8244-8248), we designed a family of novel carbenes, (Si and B)-heterocyclic carbenes (SiBHCs), and computationally demonstrated that they are stable and can bind with silver complexes to form stable (SiBHC)AgC≡CH which contain a planar tetracoordinate carbon (ptC). They can also occur Diels-Alder reactions with butadiene. Based on these novel carbenes, we further designed three porous organic molecules (POMs) and one 2D covalent organic framework (COF) whose structures and properties were studied computationally as well. We expect that this work is of general interest to the readership of MSDE.

# (Si and B)-Heterocyclic Carbenes and Theoretical Design of New Molecules

Zeqiong Tian,[a] Congjie Zhang,*[a] Zhipeng Pei,[b] Jinxia Liang*[c] and Yirong Mo*[d]

**ABSTRACT:** Using density functional theory (DFT), we theoretically designed fifteen novel and stable (Si and B)-heterocyclic carbenes (SiBHCs). While these SiBHCs are structurally similar to the B-heterocyclic carbenes (BHCs), their carbene character origins from the charge-shift (CS) bond of the inverted C=C bond. To demonstrate the applicability of these novel carbenes, we showed that they can bind with silver complexes to form (SiBHC)AgC≡CH which are thermodynamically and electronically stable and contain a planar tetracoordinate carbon (ptC). Notably, SiBHCs can go through Diels-Alder reactions with butadiene and the Diels-Alder reactions are feasible both thermodynamically and kinetically. Based on SiBHCs as $C_3$ building blocks, we further designed three porous organic molecules (POMs) and one 2D covalent organic framework (COF). The three POMs **(D1-D3)** are situated at the minima on the potential energy surfaces and contain regular hexagonal channels. The POMs are extended into 2D structures with infinite lattices to produce COF. Optimized lattice parameters of such COF (**COF-SiBHC-1**) using M06-2X functional under the periodic boundary condition (PBC) indicated that the COF is of hexagonal lattice. Thus, SiBHCs have potential applications in ptCs, organic chemistry and material design owing to their unusual geometrical and electronic structures.

## INTRODUCTION

Carbene ($CH_2$) is a highly active intermediate and has played an important role in organic chemistry.[1-10] Recognizable 'carbene' research started with the attempts by Dumas et al. to isolate and characterize methylene in 1835.[11] Carbene can be divided into Fischer- and Schrock-type carbenes according to its electronic structure. Fischer- and Schrock-type carbenes were successfully synthesized in 1964 and 1974, respectively.[12-13] Remarkably, Arduengo et al. experimentally obtained a stable N-heterocyclic carbene (NHC) in 1991.[14] Since then, NHCs have become a standing interest in experimental and theoretical domains due to their unique electronic structures and extensive applications in the fields of metal-organic chemistry[15-19] and catalysis.[20-24] Interestingly, carbenes can be produced by the isomerization of reactive intermediates $C_5H_2$ and $C_7H_2$ with a planar tetracoordinate carbon (ptC).[25-26]

Recently, we theoretically designed a new type of carbene, i.e., B-heterocyclic carbene (BHC).[27] In contrast to the structures of Fischer- and Schrock-type carbenes, the carbene characteristic of BHCs arises from a charge-shift (CS) bond.[28-31] Moreover, we found that BHCs can act as ligands and Lewis bases to form complexes with ptC.[27, 32-36] BHCs can also participate in the Diels-Alder reaction as dienophiles to generate novel [1.1.1]propellanes containing boron atom.[37-38] Additionally, BHCs were recently used to design porous organic molecules (POMs)[39] and stabilize a planar tetracoordinate silicon (ptSi).[40]

Inspired by the recent work reported by Li et al., who found that $SiH_2$ can stabilize C=N bond to produce 1-aza-2,4-disilabicyclo[1,1,0]butanes,[41] we anticipated to obtain a family of novel molecules $X_2SiC_2BR$ given by the substitution of $SiX_2$ for the $CX_2$ unit in BHCs. As such, a type of novel carbenes, (Si and B)-heterocyclic carbenes (SiBHCs) were anticipated. If the expected SiBHCs are stable, a kind of new molecules with a CS bond can be proposed as well. In addition, these SiBHCs may coordinate to transition metals as ligands and the resulting complexes should contain ptCs. These new compounds with ptCs surely would enrich the ptC chemistry proposed by Hoffmann in 1970.[42] The Diels-Alder reactions of SiBHCs with butadiene were also computationally explored. Finally, we rationally designed one kind of novel 2D covalent organic framework (COF) based on SiBHC building blocks. In contrast to COFs reported in literature,[43-45] such COFs constructed with SiBHC building blocks can serve as ligands to form metal-organic frameworks (MOFs) with ptC compounds.[39]

## COMPUTATIONAL METHODS

Previous studies of BHCs showed that the energies of BHCs are higher than those of their linear isomers, that is, the linear isomer of a BHC is more stable than the BHC itself.[35] Thus, in this work both the structures of SiBHCs and their linear isomers were studied using the density functional theory M06-2X functional[46] in combination with the 6-311G** basis set.[47] Vibrational frequencies of these molecules were calculated at the same level of theory to confirm the true minima on the potential energy surfaces. Geometry optimizations and frequency calculation of the complexes of SiBHCs coordinated to AgC≡CH were performed with the M06-2X functional and the SDD basis set[48] for Ag and the 6-311G** basis set for the rest atoms. Diels-Alder reactions of SiBHCs with butadiene

were investigated at the same M06-2X/6-311G** level. To design a 2D COF based on SiBHC building blocks, we constructed three POMs. When these POMs structures were extended into 2D structures with infinite lattices, the COF constructed by SiBHC building blocks was obtained. Both structural optimizations and frequency calculations of these POMs were performed. The COF were optimized under the periodic boundary conditions (PBCs). Wiberg bond indices (WBIs) of the most stable SiBHCs and the products of the Diels-Alder reactions of the SiBHCs with butadiene were derived by the natural bond orbital (NBO) analysis.[49] Nucleus-independent chemical shifts NICS(0) and NICS(1) at the centers of the three-membered rings formed by two C atoms and one B atom of SiBHCs were calculated by the gauge-independent atomic orbital (GIAO) method.[50] All above calculations were performed with the Gaussian09 program.[51] The AIM2000 program[52-53] was used to calculate electron density and Laplacian values of the chemical bonds of the most stable SiBHCs. Ab initio valence bond (VB) computations were carried out with XMVB.[54-56] Ab initio molecular dynamical (AIMD) simulations with the example of **B1** were carried out with the Vienna ab initio simulation package (VASP) program,[57-58] where the core and valence electrons were represented by using the projector augmented wave (PAW)[59] method and plane-wave basis functions with a kinetic energy cut-off of 400 eV. The generalized gradient approximation (GGA) with the Perdew-Burke-Ernzerhof (PBE)[60] exchange-correlation functional was used in the AIMD calculations. The finite temperature simulations of dynamical properties were performed at the temperatures 298 K and 673 K using the exact Hellman-Feynman forces and applying the statistics of the canonical ensemble to the motion of atomic nuclei by means of a Nosé thermostat.[61] Newton's equations of motion were integrated using the Verlet algorithm[62] with a time step of 1 fs. **B1** molecules were confined in the cubic box of 17*17*17 Å and a vacuum distance of more than 10 Å was set to keep the interactions between molecules in the adjacent boxes negligible. The Brillouin-zone sampling was restricted to the Γ-point. The optimization of atomic geometries was performed via a conjugate-gradient algorithm until residual forces acting on atoms were less than 0.1 eV Å$^{-1}$.

## RESULTS AND DISCUSSION

On the basis of the structures of 1-aza-2,4-disilabicyclo[1,1,0]butanes[41] and BHCs[27], we designed (Si and B)-heterocyclic carbene (SiBHC), $H_2SiC_2BH$, as illustrated in Scheme 1**a**. $H_2SiC_2BH$ (**a**) is the substitution of $SiH_2$ for the $CH_2$ unit in BHC (**b**). Scheme 1**c** illustrates the fifteen SiBHCs (X=H, R=H, Me, $NH_2$ and $NO_2$; X=F, R=H, Me, tBu, $NH_2$, $CF_3$ and $NO_2$; X=Me, R=H, Me, tBu, $NO_2$ and $B(OH)_2$). The linear isomers of SiBHCs were given in scheme 1**d**. The linear isomers of SiBHCs are formed via two isomerization paths as displayed in Scheme 1S (in Supporting Information). Optimized geometries and the relative energies of the possible structures of SiBHCs and their linear isomers were illustrated in Fig. 1S (in Supporting Information). As shown from Fig. 1S, the lowest energy structures of the fifteen SiBHCs were denoted as **Ai** (**i**=1-15) and their likely isomers as **Ai-j**. For instance, **A1** has only one linear isomer **A1-1** but **A2** has three isomers which were labelled as **A2-j** (**j**=1-3).

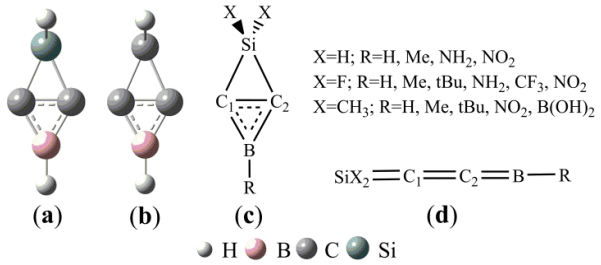


**Scheme 1.** (Si and B)-heterocyclic carbenes (SiBHCs) (**a**) and B-heterocyclic carbenes (BHCs) (**b**). Fifteen types of (Si and B)-heterocyclic carbenes (**c**) and the linear isomers (**d**).

Notably, all 15 SiBHCs (**Ai**) have significantly lower energy than their corresponding linear isomers (**Ai-j**). For example, the energies of **A1** and **A5** are lower than those of **A1-1** and **A5-1** by 30.2 and 49.0 kcal/mol, respectively. Thus, in contrast to BHCs,[35] SiBHCs are more stable compared with their linear isomers. In other words, the substitution of $SiX_2$ for the $CX_2$ unit in BHCs prefers to form SiBHCs. The energies of SiBHCs also depend upon the conformation of the groups R bonded to the boron atom in $X_2SiC_2BR$. Interestingly, **A3-1** and **A8-1** are much less stable than **A3** and **A8** by about 17.6 and 20.1 kcal/mol, respectively. The high stability of **A3** and **A8** can attribute to the conjugated π bond between B and N. Vibrational frequency calculations confirmed that all **Ai** structures situate at the minima on the potential energy surfaces. Fig. 1 shows the optimized geometries of the **Ai** for the sake of clarity.

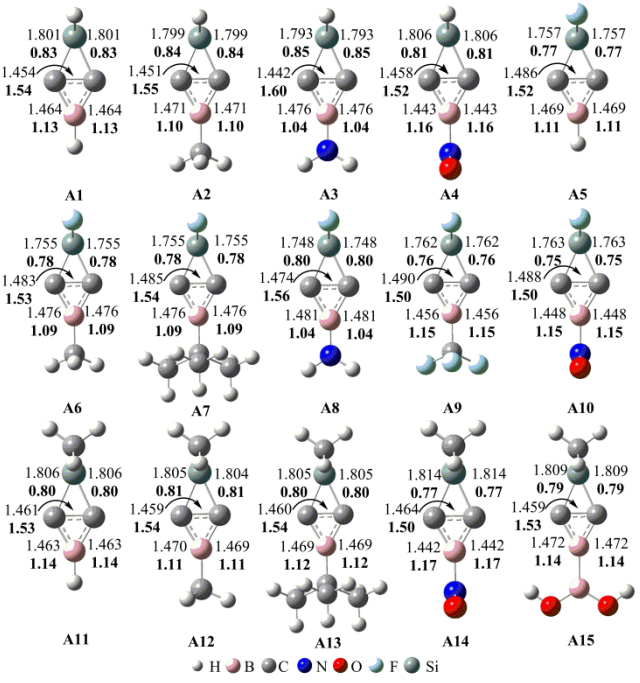

**Fig. 1.** Optimized bond lengths (in plain) and calculated WBIs (in bold) in **Ai** (**i**=1-15) at the M06-2X/6-311G** level. The bond lengths are given in Å.

As seen from Fig. 1, the distances of C-C, C-B and C-Si bonds in **Ai** (**i**=1-15) are in the ranges of 1.442~1.490, 1.442~1.481 and 1.748~1.814 Å, respectively. The lengths of C-C and C-B bonds in **Ai** are well consistent with those of BHCs.[35,37] Thus, the substitution of $SiX_2$ for the $CX_2$ unit in BHCs does not impact the chemical bonds of the three-membered ring CCB in a noticeable way. We further calculated the WBIs of C-C, C-B and C-Si bonds in **Ai** which were incorporated into Fig. 1. The WBIs of C-Si bonds in **Ai** are around 0.80, suggesting the single bond nature for the C-Si bonds. The WBIs of C-C bonds in **Ai** are in range of 1.50~1.60, thus, the C-C bonds are between single and double bonds. The WBIs of the C-B bonds in **Ai** are in the range of 1.04~1.17, indicating C-B are not classical single bonds.

To better understand the bonding nature of the C-C and C-B bonds in **Ai**, we plotted the orbitals involved in the C-C and C-B bonds in Fig. 2 and Fig. 2S (in Supporting Information). As shown in Fig. 2, the HOMOs of **Ai** are mainly the linear combination of the AOs of the two carbon atoms in the C-C bond, which are consistent with those of BHCs.[35,37] According to the π orbital and HOMO, it can be concluded that the C-C bond contains both π and CS bonds analogous to the inverted C-C bond in BHCs.[33] Fig. 2S shows an occupied π orbital extending over both carbon atoms and the boron atom, i.e. $\Pi_3^2$ with two π electrons moving over the three-membered ring (CCB). Thus, the shorter bond lengths and larger WBIs (>1.0) of the C-B bonds can be ascribed to the conjugate π orbital (aromaticity). Because the lengths, WBIs and the HOMOs are in good agreement with those of BHCs,[35,37] **Ai** (**i**=1-15) were confirmed to have carbene characteristics which origin from the charge-shift (CS) bond. As such, **Ai** can be called SiBHCs. Calculated HOMO and LUMO energies and the HOMO-LUMO gaps of **Ai** were compiled in Table 1S (in Supporting Information). The gaps between HOMO and LUMO of **Ai** are in the range of 8.23~9.20 eV, indicating **Ai** are electronically stable.

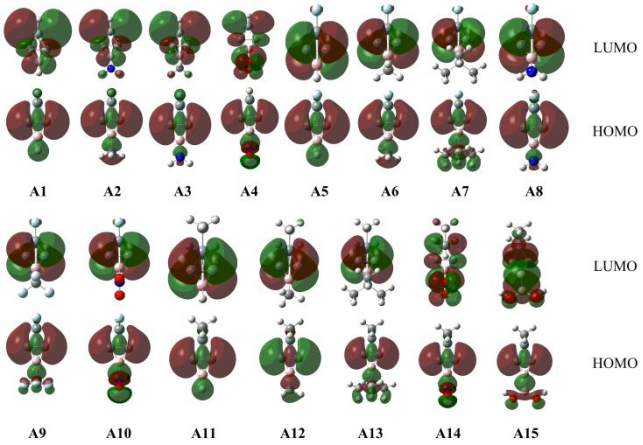


**Fig. 2.** HOMOs and LUMOs of **Ai** (**i**=1-15).

Since **Ai** (**i**=1-15) have similar structures, we employed the ab initio VB method BOVB/6-31G* to investigate the bonding of the inverted C-C bond in **A1** and verify its CS nature. **A1** can be described in terms of three resonance structures as shown in Scheme 2. Computations showed that ionic resonance structures make 34% contributions to the ground state of **A1**, suggesting that **A1** favor a carbene structure by charge-shifting. Additionally, the calculated ratios of resonance energy to bond energy for the inverted C=C bond in **A1** is 49% and meet the definition of a CS bond.

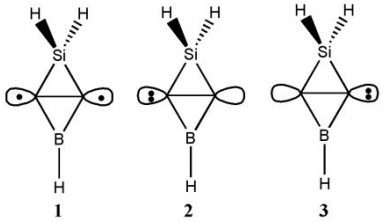


**Scheme 2**. The covalent structure (**1**) and two ionic resonance structures (**2** and **3**) arising from charge-shift over the inverted C–C bond in **A1**.

Since **Ai** (**i**=1-15) has a $\Pi_3^2$ delocalization π bond, the three-membered rings (CCB) are satisfied with the 4n+2 rule and aromatic. Accordingly, both NICS(0) and NICS(1) values in the centers of three-membered rings of **Ai** were calculated and listed in Table 2S (in Supporting Information). The NICS(0) and NICS(1) values are in the range from -38.4~-20.5 and -21.6~-11.1 ppm, respectively, indicating the strong aromaticity of these three-membered rings in **Ai**. The electron density and Laplacian values at the bond critical point (BCP) of **Ai** were calculated and listed in Table 2S (in Supporting Information). Table 2S showed that the electron densities and Laplacian values of the inverted C=C bonds were close to 0.26 and -0.37, respectively.

Similar to BHCs, the C-C bonds in **Ai** (**i**=1-15) result in the carbene characteristics for these molecules. Accordingly, we optimized the silver complexes **Bi** (**i**=1-15) which result from the coordination of **Ai** to AgC ≡ CH. Optimized geometries of these complexes were illustrated in Fig. 3. Binding energies between **Ai** and AgC≡CH, and between L(=CO, NHC) and AgC ≡ CH in complexes LAgC ≡ CH where CO or NHC coordinates to AgC ≡ CH, were calculated and compiled in Table 3S (in Supporting Information). The binding energies in the complexes LAgC ≡ CH (L=CO, NHC) were 18.4 and 45.2 kcal/mol, respectively. The binding energies in the complexes **Bi** formed by SiBHCs and AgC ≡ CH were in the range of 18.9~32.7 kcal/mol, suggesting that the formations of **Bi** are thermodynamically favorable and the coordination capability of SiBHCs ranges between CO and NHC. Frequency calculations also confirmed that **Bi** are the minima on the potential energy surfaces as they have no imaginary frequencies. The distances of ptC-Ag and Ag-C( ≡ CH) in complexes **Bi** (i=1-15) are close to 2.231 and 2.068 Å, respectively. The lengths of ptC-Ag bonds are

consistent with those of BHCs,[25] indicating that ptC-Ag bonds are coordination bonds. The short lengths of the Ag-C(≡CH) bonds in complexes **Bi** result from the ionic bond and coordination bond of the complexes AgC≡CH. The distances of ptC-B, ptC-C and ptC-Si bonds in **Bi** are close to 1.489, 1.449 and 1.838 Å, respectively, which are consistent with those of BHCs.[29] Thus, the carbon atom (ptC) in complexes **Bi** forms four bonds. In addition, the sum of the four bond angles of Si-ptC-Ag, Ag-ptC-B, B-ptC-C and C-ptC-Si in **Bi** are close to 360°, showing that the five atoms Si, C, ptC, B and Ag atoms are located on one plane. Thus, all the complexes **Bi** (i=1-15) contain ptCs.

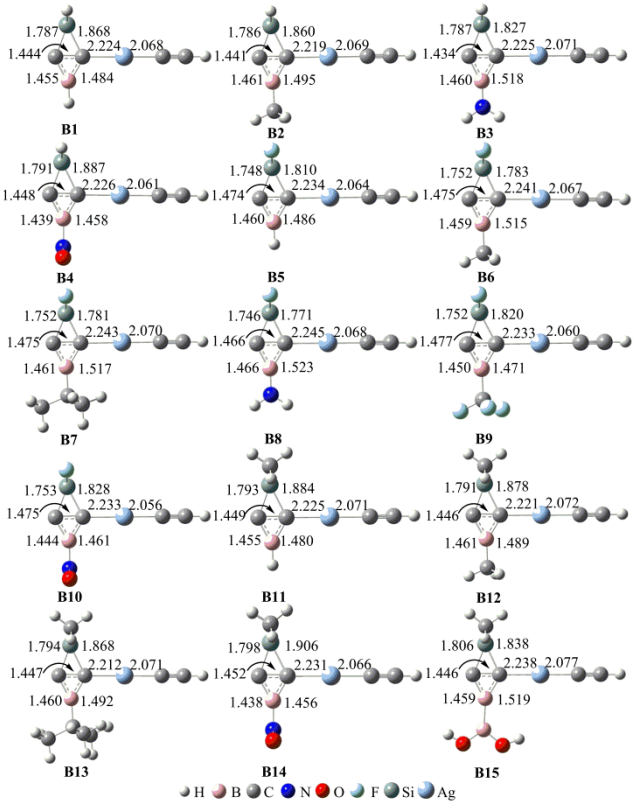


**Fig. 3** Optimized geometries of the complexes **Bi** (**i**=1-15) at the M06-2X/6-311G** level. Bond lengths (in plain) and the smallest vibrational frequencies (in italic) are given in Å and $cm^{-1}$, respectively.

To confirm the thermodynamic stability of **Bi**, ab initio molecular dynamical (AIMD) simulations of **B1** at T= 298 and 673 K were carried out and illustrated in Fig. 2S (in Supporting Information). As seen from Fig. 2S, the structure of **B1** has no significant changes at 298 K and 673 K for 8000 fs, in which the distances of Ag-C and Si-C are around 2.041 and 1.920 Å, respectively. Thus, **B1** is thermodynamically stable.

Because the LUMOs of the SiBHCs **Ai** (i=5-13) are similar to those of ethene and cyclopropane as shown in Fig. 2, these SiBHCs **Ai** (**i**=5-13) can be dienophiles to occur Diels-Alder reactions according to the frontier molecular orbital theory. The Diels-Alder reactions of **Ai** (i=5-13) with butadiene were shown in Scheme 3**a**. The transition states ($\mathbf{TS_{Ai\text{-}endo}}$ and $\mathbf{TS_{Ai\text{-}exo}}$) and products ($\mathbf{P_{Ai}}$) involved in the Diels-Alder reactions of **Ai** were illustrated in Scheme 2**b**, in which $\mathbf{TS_{Ai\text{-}endo}}$ and $\mathbf{TS_{Ai\text{-}exo}}$ were denoted in term of the orientation of $SiX_2$ unit in **Ai** toward butadiene.

Calculated reaction free energies and energy barriers of the Diels-Alder reactions of **Ai** (**i**=5-13) with butadiene were given in Fig. 4. As seen from Fig. 4**a**, the reaction free energies of the Diels-Alder reactions are in the range of -33.6~-46.7 kcal/mol, indicating these Diels-Alder reactions are thermodynamically feasible. Additionally, the electron withdrawing group X and R can result in reduced reaction free energies. For instance, the reaction free energies of **Ai** (**i**=5-10) are lower than those of **Ai** (**i**=11-13), the order of reaction free energies of **Ai** (**i**=8-10) is **A8** < **A9** < **A10**. In particular, the reaction free energy of **A10** is the lowest due to the strong withdrawing group $NO_2$.

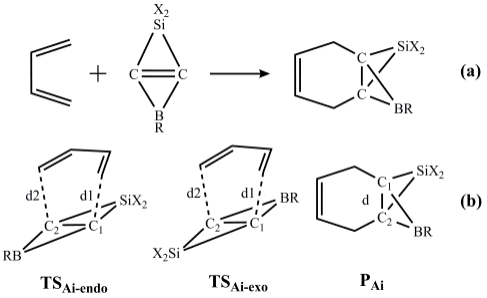


**Scheme 3** Diels-Alder reactions of SiBHCs with butadiene (**a**). Two transition states ($\mathbf{TS_{Ai\text{-}endo}}$ and $\mathbf{TS_{Ai\text{-}exo}}$) and the products ($\mathbf{P_{Ai}}$) (**b**).

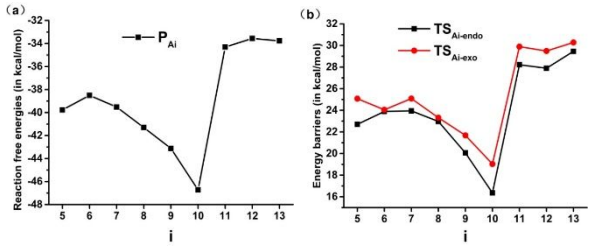


**Fig. 4** Reaction free energies (**a**) and energy barriers (**b**) of the Diels-Alder reactions of SiBHCs with butadiene.

Fig. 4**b** showed that the energy barriers of undergoing endo transition states ($\mathbf{TS_{Ai\text{-}endo}}$) are lower than those of undergoing exo transition states ($\mathbf{TS_{Ai\text{-}exo}}$). This is consistent with the reactions of cyclopropenes and BHCs with butadiene.[37-38, 63] The Diels-Alder reactions of **Ai** (**i**=5-13) via transition state $\mathbf{TS_{Ai\text{-}endo}}$ to give $\mathbf{P_{Ai}}$ with the energy barriers in the range of 16.4~29.5 kcal/mol, indicating that these Diels-Alder reactions are kinetically feasible. More interestingly, the sharpness of the energy barriers of the Diels-Alder reactions of **Ai** (**i**=5-13) is completely similar to that of the reaction free energies. Thus, the electron withdrawing group X and R substitution of SiBHCs can significantly reduce both reaction free energies and energy barriers.

Optimized bond lengths of d1 and d2 (defined in Scheme 3) in the transition structures $\mathbf{TS_{Ai\text{-}endo}}$ and $\mathbf{TS_{Ai\text{-}exo}}$ of the **Ai** (**i**=5-13) with butadiene were given in Table 4S (in Supporting Information). As seen from Table 4S, the distances of d1 and d2 in the endo and exo transition states

are in the range of 2.260~2.378 Å, and in agreement with those of cyclopropene and BHCs with butadiene.[35-36,61] Optimized distances of $C_1$-$C_2$ bonds in $\mathbf{P_{Ai}}$ (**i**=5-13) were listed in Table 5S (in supporting information). Table 5S showed that the lengths and WBIs of the inverted $C_1$-$C_2$ bond in $\mathbf{P_{Ai}}$ are around 1.770 Å and 0.75, respectively, indicating the weak interaction between $C_1$ and $C_2$.

Previous studies showed that BHCs can be $C_3$ building blocks to obtain POMs.[39] In this work, we used three **A1** and a boron atom to obtain a $C_3$ building block with the formation of B-B bonds. The $C_3$ building block have two isomers owing to the conformation of **A1**, and these two isomers (**C-1** and **C-2**) were illustrated in Fig. 5. **C-1** is formed with three coplanar **A1** monomers but in **C-2**, three **A1** monomers are perpendicular to the plane formed by four boron atoms. Optimized geometries, relative energies, and the number of imaginary frequencies of **C-1** and **C-2** were presented in Fig. 5. **C-2** is more stable than **C-1** by 24.8 kcal/mol and has no imaginary frequency. Based on **C-2**, we constructed three POMs by forming Si-Si bonds. Optimized geometries of three POMs were displayed in Fig. 6. The lengths of the edges of the hexagonal channels in these POMs (**D1-D3**) are about 10.56 Å. Thus, the hexagonal channels in **D1-D3** are regular hexagons, in which the apertures of the hexagonal channels are about 13.9 Å.

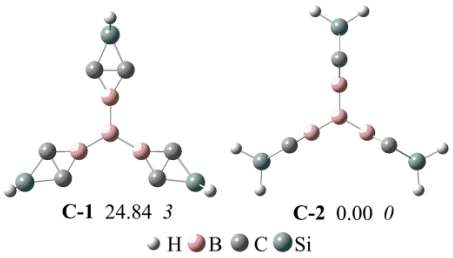


**Fig. 5** Optimized structures, relative energy (in plain) and the number of imaginary frequency (in italic) of **C-1** and **C-2** at the M06-2X/6-311G** level. The relative energies are given in kcal/mol.

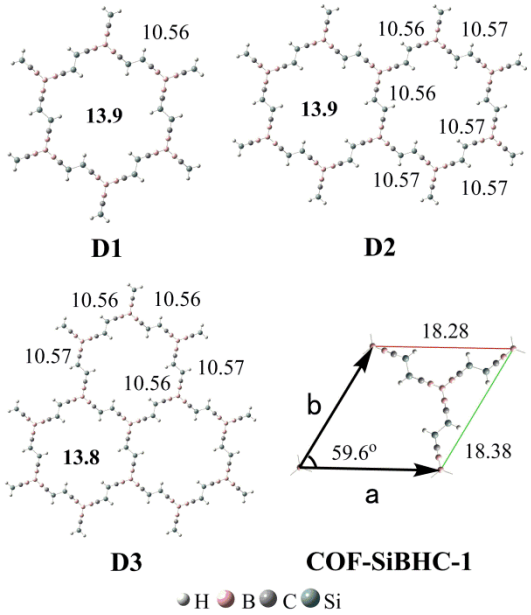


**Fig. 6** Optimized side lengths (in plain) and apertures (in bold) of **D1-D3** and lattice parameters (in plain) of **COF-SiBHC-1**. The side lengths, apertures and lattice parameters are given in Å.

When the structures of **D1-D3** were extended to 2D structures with infinite lattices, one kind of COF could be produced. Optimized lattice parameters of this COF (**COF-SiBHC-1**) using the M06-2X functional under the PBC were also illustrated in Fig. 6. The three lattice parameters (**a**, **b** and the angle between **a** and **b**) of **COF-SiBHC-1** are 18.28 Å, 18.38 Å and 59.6°, respectively. Thus, such 2D COF formed by SiBHCs is a hexagonal lattice. The apertures of the hexagonal channels of **COF-SiBHC-1** are about 13.9 Å.

## CONCLUSIONS

Based on the DFT computations, we rationally designed and theoretically predicted fifteen novel and stable SiBHCs derived from the substitution of $SiX_2$ for the $CX_2$ unit in B-heterocyclic carbenes (BHCs). SiBHCs at the singlet state were found to be lowest energy structures. The carbene characters of the SiBHCs result from the CS bond of the C-C bonds in SiBHCs, analogous to BHCs. The NICS(0) and NICS(1) values at the centers of the three-membered rings covered CCB atoms of SiBHCs confirmed that SiBHCs are aromatic compounds. The binding energies of the complexes of SiBHCs with AgC≡CH indicated that the formation of (SiBHC)AgC≡CH would be thermodynamically favorable, in which the complexes of (SiBHC)AgC≡CH contain ptCs. These (SiBHC)AgC≡CH represent a new family of carbenes for designing complexes with ptCs. Computations also confirmed that the Diels-Alder reactions of the SiBHCs **Ai** (i=5-13) with butadiene are feasible both thermodynamically and kinetically. These Diels-Alder reactions prefer endo transition states to give products. Finally, we designed three POMs and one kind of novel 2D COF based on SiBHCs building blocks, in which the structures of **D1-D3**

are extended into 2D structures with infinite lattices to give 2D COF. The symmetry of 2D COF (**COF-SiBHC-1**) is approximately hexagonal, in which the apertures of the hexagonal channels of **COF-SiBHC-1** are about 13.9 Å. We anticipate that these SiBHCs have potential applications in metal organic chemistry and material design due to their unusual structure and stability if they were isolated experimentally.

## ASSOCIATED CONTENT

Supporting Information
Scheme 1S; Fig. 1S to 3S; Tables 1S-5S; Cartesian coordinates, electronic energy (E) and the smallest vibrational frequency (v) of **Ai** (i=1-15), **Bi** (i=1-15), butadiene, $\mathbf{P_{Ai}}$ (i=5-13), $\mathbf{TS_{Ai\text{-}endo}}$ (i=5-13), $\mathbf{TS_{Ai\text{-}exo}}$ (i=5-13), **C-1, C-2** and **D1-D3.** Cartesian coordinates, electronic energy (E) of **COF-SiBHC-1**.

## AUTHOR INFORMATION

### Corresponding Authors

[a] Congjie Zhang– Key Laboratory of Macromolecular Science of Shaanxi Province, School of Chemistry & Chemical Engineering, Shaanxi Normal University, Xi'an, 710062, China; E-mail: zcjwh@snnu.edu.cn

[b] Jinxia Liang– School of Chemistry and Chemical Engineering, Guizhou University, Guiyang 550025, China; E-mail: liangjx2009@163.com

[d] Yirong Mo– Department of Nanoscience, Joint School of Nanoscience and Nanoengineering, University of North Carolina at Greensboro, Greensboro, NC 27401, USA. E-mail: y_mo3@uncg.edu

### Authors

[a] Zeqiong Tian– Key Laboratory of Macromolecular Science of Shaanxi Province, School of Chemistry & Chemical Engineering, Shaanxi Normal University, Xi'an, 710062, China.

[b] Zhipeng Pei– Institute for Nanoscale Science and Technology, College of Science and Engineering, Flinders University, Adelaide, South Australia 5042, Australia.

### Notes

The authors declare no competing financial interest.

## ACKNOWLEDGMENT

The authors thank the National Natural Science Foundation of China for financial support (No. 21373133). This work was performed in part at the Joint School of Nanoscience and Nanoengineering, a member of the Southeastern Nanotechnology Infrastructure Corridor (SENIC) and National Nanotechnology Coordinated Infrastructure (NNCI), which is supported by the National Science Foundation (Grant ECCS-2025462).

## REFERENCES

1 A. J. Arduengo, H. V. R. Dias, J. C. Calabrese and F. Davidson, *Organometallics*, 1993, **12**, 3405-3409.

2 A. J. Arduengo, F. Davidson, H. V. R. Dias, J. R. Goerlich, D. Khasnis, W. J. Marshall and T. K. Prakasha, *J. Am. Chem. Soc.*, 1997, **119**, 12742-12749.

3 X.-Y. Yu, B. O. Patrick and B. R. James, *Organometallics*, 2006, **25**, 2359-2363.

4 A. J. Arduengo and G. Bertrand, *Chem. Rev.*, 2009, **109**, 3209-3210.

5 J. A. Flores, N. Komine, K. Pal, B. Pinter, M. Pink, C.-H. Chen, K. G. Caulton and D. J. Mindiola, *ACS Catal.*, 2012, **2**, 2066-2078.

6 T. Sainsbury, M. Passarelli, M. Naftaly, S. Gnaniah, S. J. Spencer and A. J. Pollard, *ACS Appl. Mater. Interfaces*, 2016, **8**, 4870-4877.

7 A. D. Dilman and V. V. Levin, *Acc. Chem. Res.*, 2018, **51**, 1272-1280.

8 R. Nakano, R. Jazzar and G. Bertrand, *Nat. Chem.*, 2018, **10**, 1196-1200.

9 G. K. Ramollo, I. Strydom, M. A. Fernandes, A. Lemmerer, S. O. Ojwach, J. L. van Wyk and D. I. Bezuidenhout, *Inorg. Chem.*, 2020, **59**, 4810-4815.

10 F. Vermersch, S. Yazdani, G. P. Junor, D. B. Grotjahn, R. Jazzar and G. Bertrand, *Angew. Chem. Int. Ed.*, 2021, **60**, 27253-27257.

11 J. B. Dumas and E. Peligot, *Ann. Chim. Phys.*, 1835, **58**, 5-74.

12 E. O. Fischer and A. Maasböl, *Angew. Chem. Int. Ed.*, 1964, **3**, 580-581.

13 R. R. Schrock, *J. Am. Chem. Soc.*, 1974, **96**, 6796-6797.

14 A. J. Arduengo, R. L. Harlow and M. Kline, *J. Am. Chem. Soc.*, 1991, **113**, 361-363.

15 L. J. Xu, W. P. Chen and J. L. Xiao, *Organometallics*, 2000, **19**, 1123-1127.

16 N. Marion, O. Navarro, J. G. Mei, E. D. Stevens, N. M. Scott and S. P. Nolan, *J. Am. Chem. Soc.*, 2006, **128**, 4101-4111.

17 H. S. Yao, J. G. Zhang, Y. Zhang, H. M. Sun and Q. Shen, *Organometallics*, 2010, **29**, 5841-5846.

18 S. P. Desai, M. Mondal and J. Choudhury, *Organometallics*, 2015, **34**, 2731-2736.

19 H. Y. Zhang, R. Yuan, J. S. Song, X. Y. Li, Y. L. Zeng and Y. R. Mo, *Organometallics*, 2020, **39**, 3240-3249.

20 M. G. Gardiner, W. A. Herrmann, C.-P. Reisinger, J. Schwarz and M. Spiegler, *J. Organomet. Chem.*, 1999, **572**, 239-247.

21 M. Poyatos, J. A. Mata and E. Peris, *Chem. Rev.*, 2009, **109**, 3677-3707.

22 A. Patra, S. Mukherjee, T. K. Das, S. Jain, R. G. Gonnade and A. T. Biju, *Angew. Chem. Int. Ed.*, 2017, **56**, 2730-2734.

23 C. Dutta, S. S. Rana and J. Choudhury, *ACS Catal.*, 2019, **9**, 10674-10679.

24 J. Jeong, J. Heo, D. Kim and S. Chang, *ACS Catal.*, 2020, **10**, 5023-5029.

25 A. Karton and V. S. Thimmakondu, *J. Phys. Chem. A* 2022, **126**, 2561–2568.

26 K. Thirumoorthy, A. Karton, and V. S. Thimmakondu, *J. Phys. Chem. A* 2018, **122**, 9054–90641

27 C. J. Zhang and F. F. Li, *J. Phys. Chem. A*, 2012, **116**, 9123-9130.

28 S. Shaik, Z. H. Chen, W. Wu, A. Stanger, D. Danovich and P. C. Hiberty, *ChemPhysChem*, 2009, **10**, 2658-2669.

29 W. Wu, J. J. Gu, J. S. Song, S. Shaik and P. C. Hiberty, *Angew. Chem. Int. Ed.*, 2009, **48**, 1407-1410.

30 S. Shaik, D. Danovich, W. Wu and P. C. Hiberty, *Nat. Chem.*, 2009, **1**, 443-449.

31 S. Shaik, D. Danovich, W. Wu, P. F. Su, H. S. Rzepa and P. C. Hiberty, *Nat. Chem.*, 2012, **4**, 195-200.

32 C. J. Zhang, H. Zhao and J. X. Li, *Comput. Theor. Chem.*, 2015, **1054**, 22-28.

33 S. N. Yang and C. J. Zhang, *J. Phys. Chem. A*, 2015, **119**, 8950-8957.

34 X. F. Jia and C. J. Zhang, *Comput. Theor. Chem.*, 2016, **1075**, 47-53.

35 C. J. Zhang, D. X. Ma, S. N. Yang and J. X. Liang, *ACS Omega*, 2016, **1**, 620-625.

36 C. J. Zhang, F. Fan, Z. M. Wang, J. S. Song, C. S. Li and Y. R. Mo, *Chem. – Eur. J.*, 2018, **24**, 10216-10223.

37 C. J. Zhang, Z. M. Wang, J. S. Song, C. S. Li and Y. R. Mo, *Theor. Chem. Acc.*, 2019, **138**, 106.

38 C. J. Zhang, H. Jiao and W. H. Jia, *Comput. Theor. Chem.*, 2020, **1175**, 112734.

39 C. J. Zhang, Z. Q. Tian, W. H. Jia and Y. R. Mo, *Mol. Syst. Des. Eng.*, 2021, **6**, 132-138.

40 C. J. Zhang, Z. Q. Tian and W. H. Jia, *J. Phys. Chem. A*, 2021, **125**, 843-847.

41 J. C. Li, D. J. Goffitzer, M. Y. Xiang, Y. L. Chen, W. J. Jiang, M. Diefenbach, H. P. Zhu, M. C. Holthausen and H. W. Roesky, *J. Am. Chem. Soc.*, 2021, **143**, 8244-8248.

42 R. Hoffmann, R. W. Alder and C. F. Wilcox, *J. Am. Chem. Soc.*, 1970, **92**, 4992-4993.

43 A. P. Côté, A. I. Benin, N. W. Ockwig, M. O'Keeffe, A. J. Matzger and O. M. Yaghi, *Science*, 2005, **310**, 1166-1170.

44 P. Kuhn, M. Antonietti and A. Thomas, *Angew. Chem. Int. Ed.*, 2008, **47**, 3450-3453.

45 F. J. Uribe-Romo, J. R. Hunt, H. Furukawa, C. Klöck, M. O'Keeffe and O. M. Yaghi, *J. Am. Chem. Soc.*, 2009, **131**, 4570-4571.

46 Y. Zhao and D. G. Truhlar, *Theor. Chem. Acc.*, 2008, **120**, 215-241.

47 R. Krishnan, J. S. Binkley, R. Seeger and J. A. Pople, *J. Chem. Phys.*, 1980, **72**, 650-654.

48 D. Andrae, U. Häußermann, M. Dolg, H. Stoll and H. Preuß, *Theor. Chim. Acta*, 1990, **77**, 123-141.

49 E. D. Glendening, J. K. Badenhoop, A. E. Reed, J. E. Carpenter, J. A. Bohmann, C. M. Morales and F. Weinhold, *NBO Version 5.0*, Theoretical Chemistry Institute, University of Wisconsin, Madison, WI, 2001.

50 P. v. R. Schleyer, C. Maerker, A. Dransfeld, H. J. Jiao and N. J. R. van Eikema Hommes, *J. Am. Chem. Soc.*, 1996, **118**, 6317-6318.

51 M. J. Frisch, G. W. Trucks, H. B. Schlegel, G. E. Scuseria, M. A. Robb, J. R. Cheeseman, G. Scalmani, V. Barone, B. Mennucci, G. A. Petersson, H. Nakatsuji, M. Caricato, X. Li, H. P. Hratchian, A. F. Izmaylov, J. Bloino, G. Zheng, J. L. Sonnenberg, M. Hada, M. Ehara, K. Toyota, R. Fukuda, J. Hasegawa, M. Ishida, T. Nakajima, Y. Honda, O. Kitao, H. Nakai, T. Vreven, J. A. Montgomery, Jr., J. E. Peralta, F. Ogliaro, M. Bearpark, J. J. Heyd, E. Brothers, K. N. Kudin, V. N. Staroverov, T. Keith, R. Kobayashi, J. Normand, K. Raghavachari, A. Rendell, J. C. Burant, S. S. Iyengar, J. Tomasi, M. Cossi, N. Rega, J. M. Millam, M. Klene, J. E. Knox, J. B. Cross, V. Bakken, C. Adamo, J. Jaramillo, R. Gomperts, R. E. Stratmann, O. Yazyev, A. J. Austin, R. Cammi, C. Pomelli, J. W. Ochterski, R. L. Martin, K. Morokuma, V. G. Zakrzewski, G. A. Voth, P. Salvador, J. J. Dannenberg, S. Dapprich, A. D. Daniels, O. Farkas, J. B. Foresman, J. V. Ortiz, J. Cioslowski and D. J. Fox, *Gaussian 09*, Revision D.01; Gaussian, Inc., Wallingford CT, 2013.

52 F. Biegler-König, J. Schönbohm and D. Bayles, *J. Comput. Chem.*, 2001, **22**, 545-559.

53 F. Biegler-König and J. Schönbohm, *J. Comput. Chem.*, 2002, **23**, 1489-1494.

54 L. Song, Z. Chen, F. Ying, J. Song, X. Chen, P. Su, Y. Mo, Q. Zhang, W. Wu, XMVB 2.1: an ab initio non-orthogonal valence bond program. 2015, Xiamen University, Xiamen.

55 L. Song, Y. Mo, Q. Zhang, W. Wu, *J. Comput. Chem.*, 2005, **26**, 514–521.

56 W. Wu, P. Su, S. Shaik, P. C. Hiberty, Chem. Rev., 2011, **111**, 7557–7593.

57 G. Kresse, J. Hafner, *Phys. Rev. B*, 1993, **47**, 558–561.

58 G. Kresse, D. Joubert, *Phys. Rev. B*, 1999, **59**, 1758–1775.

59 P. E. Blöchl, *Phys. Rev. B*, 1994, **50**, 17953–17979.

60 J. P. Perdew, K. Burke, M. Ernzerhof, *Phys. Rev. Lett.* 1996, **77**, 3865–3868.

61 S. Nosé, *J. Chem. Phys*. 1984, **81**, 511–519.

62 L. Verlet, *Phys. Rev*. 1967, **159**, 98–103

63 B. J. Levandowski and K. N. Houk, *J. Am. Chem. Soc.*, 2016, **138**, 16731-16736.